Emission Spectra and Electronic Energy Levels of the Rotational Isomers of Pyridinecarboxaldehyde Vapors

Takao Itoh†

Graduate School of Integrated Arts and Science, Hiroshima University, 1-7-1 Kagamiyama, Higashi-Hiroshima City, 739-8521 Japan

Received: March 29, 2006

Emission and excitation spectra of 2-, 3- and 4-pyridinecarboxaldehyde (2-, 3- and 4-PCA, respectively) vapors have been measured at different temperatures and compared to one another. The emission spectra of these vapors are shown to consist of the $T_1(n, \pi^*) \rightarrow S_0$ phosphorescence accompanied by the weak thermally activated $S_1(n, \pi^*) \rightarrow S_0$ delayed fluorescence. Two peaks originating from the two rotamers (syn and anti) have been identified in the fluorescence, phosphorescence and excitation spectra of 3-PCA vapor. Analyses of the temperature dependence and vibrational structure of the spectra of 3-PCA vapor provide the syn−anti energy difference of 190 ± 30 cm^{-1} in the T_1 (n, π^*) state, 200 ± 30 cm^{-1} in the S_1(n, π^*) state, and 290 ± 35 cm^{-1} in the ground state. The ground-state energy difference is in agreement with the result of density functional theory (DFT) calculation for 3-PCA vapor. DFT calculation demonstrated also that the syn rotamer exists as a less stable isomer in the ground state for 2- and 3-PCA vapors.

1. Introduction

It is generally not easy to identify the rotational isomers (rotamers) spectroscopically and to investigate the dynamical behavior of each rotamer in the ground and excited states, because the electronic energy levels of the rotamers are normally located closely to one another. There are two stable planar rotamers, anti (O-trans) and syn (O-cis), for 2- and 3-pyridinecarboxaldehyde (2-PCA and 3-PCA, respectively) among three structural isomers, 2-, 3- and 4-PCA (Figure 1). The presence of the two rotamers has been indicated not only by NMR and dipole moment measurements[1−4] but also by ab initio calculation using the minimal STO-3G basis set[5] for 2- and 3-PCA. However, the definite spectroscopic identification and assignments have not been made for the two rotamers of 2- and 3-PCA. Further, detailed information on the vapor-phase emission is not available for pyridinecarboxaldehydes, although there are several other spectroscopic data in the literature.[6−12] Thus, it is of interest to obtain a deeper insight into the energetics and dynamical behavior of each rotamer in the ground and excited states through the emission spectral measurements in the vapor phase. Although supersonic-jet experiments provide information on the excited states of cooled and collision-free molecules, it is normally not easy to obtain the highly resolved phosphorescence spectra and to investigate the temperature dependence of the spectra in a jet.

In the present work, the emission and excitation spectra of 2-, 3- and 4-PCA vapors have been measured in the presence of a buffer gas at different temperatures. The emission spectra of pyridinecarboxaldehyde vapors are shown to consist of the $T_1(n, \pi^*) \rightarrow S_0$ phosphorescence accompanied by the weak thermally activated $S_1(n, \pi^*) \rightarrow S_0$ delayed fluorescence. The S_1-T_1 energy separations obtained from the temperature dependence of the emission spectra agreed well with those obtained from the band positions for all the molecules. Two peaks originating from the two different rotamers have been identified in the fluorescence, phosphorescence and excitation spectra of 3-PCA vapor. Temperature dependence of the phosphorescence and phosphorescence excitation spectra of 3-PCA vapor, along with the observed band positions, provides the syn−anti energy difference of 190 ± 30 cm^{-1} in the T_1 (n, π^*) state, 200 ± 30 cm^{-1} in the S_1 state, and 290 ± 35 cm^{-1} in the ground state. The energy difference in the ground state is in good agreement with that obtained from DFT calculation,

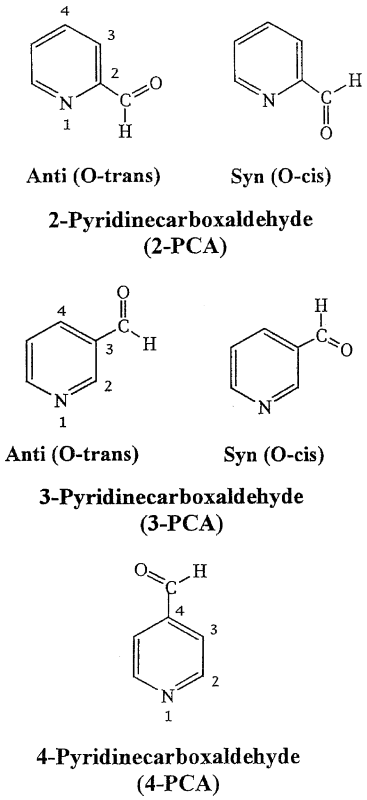

Figure 1. Molecular structures of 2-, 3- and 4-pyridinecarboxaldehyde.

† E-mail address: titoh@hiroshima-u.ac.jp.

10.1021/jp068043a CCC: $33.50
Published on Web 08/02/2006

which demonstrated also that the higher-energy peaks in the phosphorescence and excitation origins originate from the anti rotamer for 3-PCA. With 2-PCA, vibrational analysis of the phosphorescence spectrum and DFT calculation demonstrated that the observed emission originates exclusively from the anti rotamer.

2. Experimental and Computational Methods

2-, 3- and 4-PCA obtained from Aldrich, USA were purified by means of trap-to-trap distillations under vacuum. The absence of any impurity emission in glassy matrix at 77 K and verification that the phosphorescence excitation spectra in the vapor phase agreed well with the corresponding absorption spectra suggest that the purified samples were sufficiently pure for the experiment. Perfluorohexane obtained from Aldrich, USA was used as a buffer gas. The samples were carefully degassed by repeating freeze−thaw cycles in an all-glass made vacuum system equipped with a diffusion pump. The sample pressures were always kept blow the saturation pressures at the temperatures used in the present study. In the present experiment, a buffer gas was added to the samples, because the emission of the samples is weak without buffer gas and because addition of buffer gas induces the efficient collisional relaxation. The more details of the sample preparation are described in a foregoing paper.[13] Because all the samples were found to be extremely unstable with respect to photon irradiation, all the measurements were carried out only once for each fresh sample just after the preparation. In most of the spectral measurements, square 10 mm path length quartz cells were used and the temperature of the cell was controlled by a thermostated cell holder.

Absorption spectra were measured with a Shimadzu UV-2550 spectrophotometer and the emission and excitation spectra were measured with a Spex Fluorolog-3 (Model 21-SS) spectrophotometer. The latter photometer, designed especially for the measurements of weak emission signals, is equipped with a double-grating excitation monochromator, a high-pressure 450 W Xenon lamp as an excitation-light source and a photomultiplier tube (Hamamatsu R928-P) in an electric-cooled housing operated in photon-counting mode to detect weak signals. In most of the spectral measurements, the silt width was kept near 2.5 Å (12.3 cm^{-1} at 450 nm) and the wavelength calibration was carried out using a Melles Griot He−Ne green laser (5435 Å).

Quantum chemical calculations were carried out not only with the density-functional theory (DFT) using GAUSSIAN 03 program[14] but also with semiempirical SCF-MO methods at MNDO, AMI and PM3 levels included in a MOPAC package.[15] Optimized geometries, total energies and harmonic wavenumbers in the ground state were obtained by DFT calculations using the 6-311++G(3df,2pd) basis set, Becke's three-parameter exchange functional[16] and the correlation functionals of Lee−Yang−Parr (B3LYP).[17]

3. Results and Discussion

3.1. Emission Spectra of 2- and 4-Pyridinecarboxaldehyde Vapors. Figures 2a and 3a show respectively the emission spectra of 2- and 4-PCA vapors at different temperatures in the presence of 280 Torr perfluorohexane. These spectra exhibit prominent temperature dependence: The intensity of the weak band at near 26 300 cm^{-1} relative to the strong band at near 24 400 cm^{-1} increases with increasing temperature. Further, the former and latter emission bands correspond well to the $S_0 \rightarrow S_1(n, \pi^*)$ and the $S_0 \rightarrow T_1(n, \pi^*)$ excitation origins, respectively,

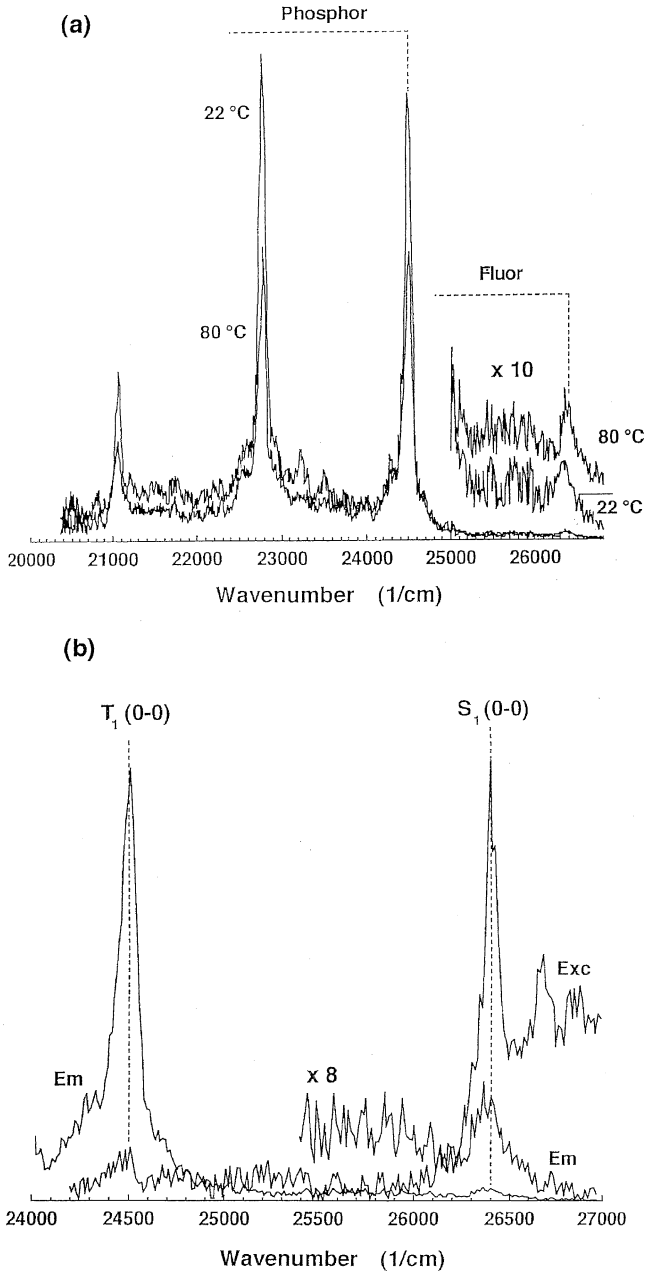

Figure 2. (a) Emission spectra of 2-PCA vapor in the presence of 280 Torr perfluorohexane at two different temperatures. (b) Emission and excitation spectra of 2-PCA vapor in the presence of perfluorohexane in an expanded scale, where the emission and excitation spectra are measured at 80 and 19 °C, respectively.

as shown in Figures 2b and 3b. These spectral features are exactly the same as those of the $T_1(n, \pi^*)$ phosphorescence and thermally activated $S_1(n, \pi^*)$ delayed fluorescence observed for benzaldehyde vapor.[18] Thus, the emission peak at near 26 300 and 24 400 cm^{-1} can be assigned respectively to the $S_1(n, \pi^*)$ delayed fluorescence and $T_1(n, \pi^*)$ phosphorescence origins.

To confirm this assignment, the relative emission intensities have been analyzed quantitatively. When two closely located electronic states are in thermodynamic equilibrium, the quantum yield ratio of the emission from the lower state (T_1) to that from the upper state (S_1), Φ_P/Φ_F, is given approximately by $\Phi_P/\Phi_F = (k_P/k_F) \times \exp[\Delta E_{S-T}/kT]$, where ΔE_{S-T} is the S_1-T_1 energy separation, and k_F and k_P are respectively the radiative rate constants of the S_1 and T_1 states. We have used the integrated intensities of the fluorescence and phosphorescence origin bands subtracted by the background intensities, I_F and I_P, respectively,

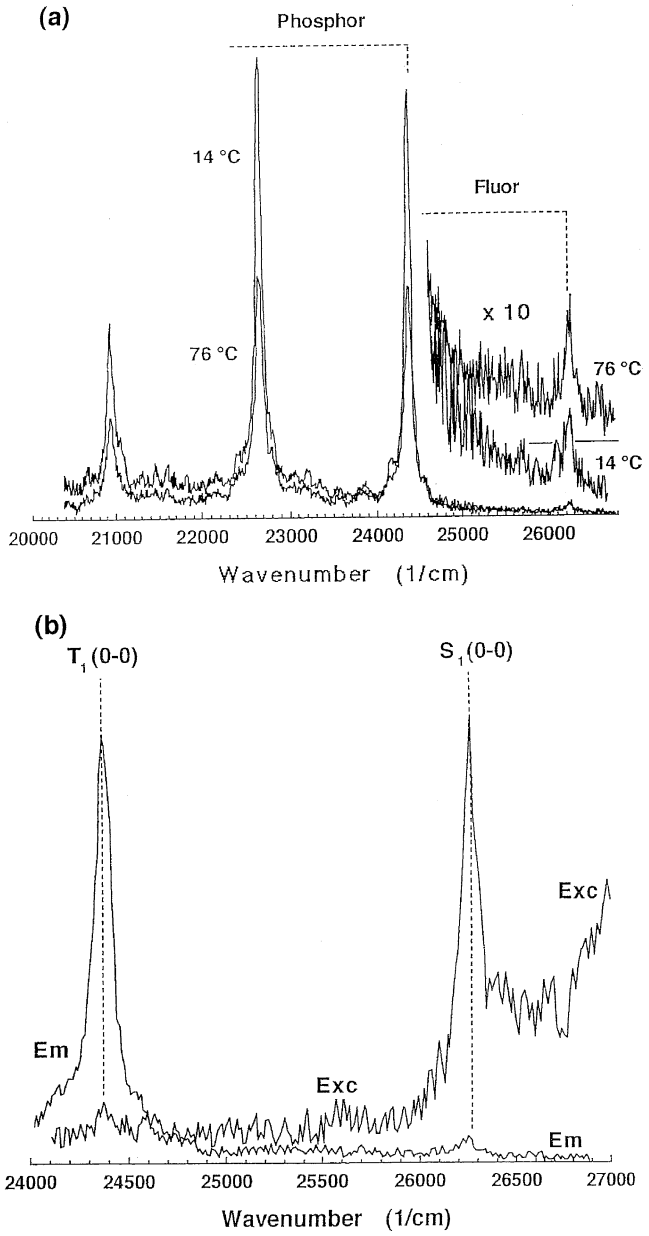

Figure 3. (a) Emission spectra of 4-PCA vapor in the presence of 280 Torr perfluorohexane at two different temperatures. (b) Emission and excitation spectra of 4-PCA vapor in the presence of perfluorohexane in an expanded scale, where the emission and excitation spectra are measured at 76 and 67 °C, respectively.

instead of Φ_F and Φ_P. Temperature dependence of I_P/I_F is shown in Figure 4. The ΔE_{S-T} and k_P/k_F values obtained from the logarithmic plots of I_P/I_F versus I/T are respectively 1800 ± 50 cm^{-1} and 8.2 × 10^{-3} for 2-PCA and 1730 ± 150 cm^{-1} and 9.5 × 10^{-3} for 4-PCA. The S_1 fluorescence and T_1 phosphorescence origins of 2-PCA vapor are observed at 26 380 and 24 510 cm^{-1}, respectively, indicating the ΔE_{S-T} value of 1870 cm^{-1}. With 4-PCA vapor, the fluorescence origin and the phosphorescence origins are observed respectively at 26 235 and 24 375 cm^{-1}. Thus, the ΔE_{S-T} value of 4-PCA vapor is evaluated to be 1860 cm^{-1}, which agrees well with that observed in a jet (1864 cm^{-1}).[12] Hence, the ΔE_{S-T} values estimated from the temperature dependence of the emission spectra are in reasonable agreement with those determined from the band positions for 2- and 4-PCA vapors. The obtained k_P/k_F values are also in reasonable agreement with the $S_0 \rightarrow T_1/S_0 \rightarrow S_1$ origin-band intensity ratio of the absorption spectra in hexane (1.4 × 10^{-2} for both 2- and 4-PCA).[19]

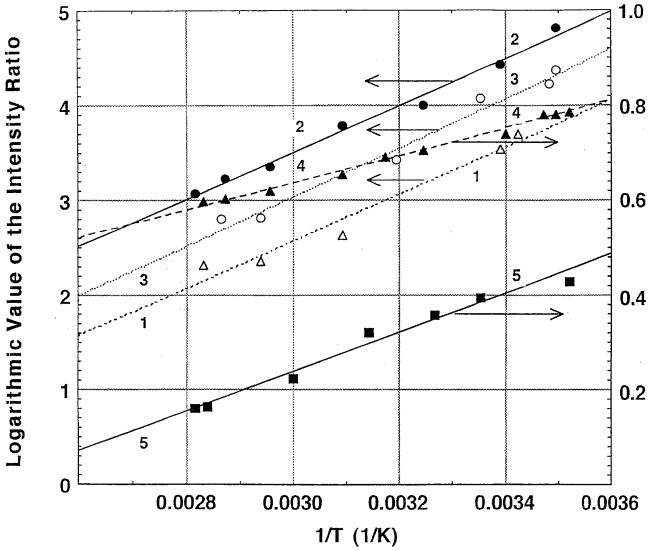

Figure 4. Logarithmic values of I_P/I_F plotted against 1/T for 2-, 3- and 4-PCA vapors (1−3, respectively), and those of the intensity ratios of the two peaks in the phosphorescence origin, I(24725 cm^{-1})/I(24825 cm^{-1}) (4), and in the S_1 excitation origin, I(26535 cm^{-1})/I(26450 cm^{-1}) (5), plotted against I/T for 3-PCA vapor.

TABLE 1: Band Locations and Assignments of the Emission Spectrum of 2-PCA Vapor (Anti)

frequency (cm^{-1})[a]	intensity[b]	assignment[c]	infrared[d]
26380	w	S_1(0−0), anti	
24510	vs	T_1(0−0), anti	
24290	m	220	215, 217[e]
23505	m	1005	1008
23290	m	1220	1219
23210	m	1300	1298, 1304
22925	m	1585	1583, 1589
22785	vs	1725	1726
22565	m	1725 + 220	
21780	m	1725 + 1005	
21065	vs	1725 × 2	

[a] The band locations have been determined with an accuracy of ±5 cm^{-1}. [b] vs, very strong; s, strong; m, medium; w, weak. [c] Only the vibrational frequencies in the ground state are indicated. As for vibrational assignments, see ref 19. [d] In Ar matrix at 13 K. [e] Obtained by DFT calculations, with the modification that the harmonic wavenumbers ν_{harm} were scaled by the relation, $\nu_{calc} = \nu_{harm} \times (0.9766 + 0.00000202 \times \nu_{harm})$, to reproduce the observed spectra (Yoshida, H.; Takeda, K.; Okamura, J.; Ehara, A.; Matsuura, H. *J. Phys. Chem. A* **2002**, *106*, 3580).

DFT calculation for 2-PCA in the ground state demonstrated that the anti rotamer is more stable than the syn rotamer by 1396 cm^{-1}, which leads to the syn/anti population ratio of 0.003/1 at 80 °C. This indicates that neither the $S_0 \rightarrow T_1$ nor $S_0 \rightarrow S_1$ transition of the syn rotamer of 2-PCA vapor is detectable in the excitation spectrum even at temperatures as high as 80 °C. The band assignments for the emission spectra of 2- and 4-PCA vapors are summarized in Tables 1 and 2. Almost all the observed emission bands of 2-PCA vapor can be assigned by considering only those from the anti rotamer, indicting that the observed emission originates exclusively from the anti rotamer. The fundamental frequency of the C═O stretching mode in the phosphorescence spectra is found to be 1725 cm^{-1} for both 2- and 4-PCA vapors, which agrees well with the infrared data obtained in Ar matrix (1726 and 1725 cm^{-1} for 2- and 4-PCA, respectively).[19]

TABLE 2: Band Locations and Assignments of the Emission Spectrum of 4-PCA Vapor

frequency (cm^{-1})[a]	intensity[b]	assignment[c]	infrared[d]
26235	w	$S_1(0-0)$	
24375	vs	$T_1(0-0)$	
24160	m	215	210, 220[e]
23895	m	480	476[e]
23575	m	800	801
23540	m	835	835
23370	m	1005	1004
23175	m	1200	1191, 1216
23055	m	1320	1322
22795	m	1580	1570
22650	vs	1725	1725
22440	m	1725 + 210	
22170	m	1725 + 480	
21815	m	1725 + 835	
21450	m	1725 + 1200	
20935	vs	1725 × 2	

[a] The band locations have been determined with an accuracy of ±5 cm^{-1}. [b] vs, very strong; s, strong; m, medium; w, weak. [c] Only the vibrational frequencies in the ground state are indicated. As for vibrational assignments, see ref 19. [d] In Ar matrix at 13 K. [e] Obtained by DFT calculations, with the modification that the harmonic wavenumbers ν_{harm} were scaled by the relation, $\nu_{calc} = \nu_{harm} \times (0.9766 + 0.00000202 \times \nu_{harm})$, to reproduce the observed spectra (Yoshida, H.; Takeda, K.; Okamura, J.; Ehara, A.; Matsuura, H. *J. Phys. Chem. A* **2002**, *106*, 3580).

3.2. Emission Spectra and Dynamics of the Two Rotamers of 3-PCA Vapor. Figure 5a shows the emission spectra of 3-PCA vapor measured at different temperatures in the presence of 280 Torr perfluorohexane. As in the case of 2- and 4-PCA vapors, the emission consists of the weak fluorescence from $S_1(n, \pi^*)$ and the strong phosphorescence from $T_1(n, \pi^*)$, showing a characteristic progression in the C═O stretching vibration. Further, the weak fluorescence exhibits the temperature dependence peculiar to the thermally activated delayed fluorescence. Closer inspection of the spectra reveals two peaks separated by 100 cm^{-1} near the phosphorescence origin and those separated by 85 cm^{-1} near the $S_0 \rightarrow S_1(n, \pi^*)$ excitation origin. The stronger phosphorescence peak at 24 825 cm^{-1} agrees in position with the $S_0 \rightarrow T_1(n, \pi^*)$ excitation origin (Figure 5b). The excitation peak corresponding to the lower phosphorescence peak at 24 725 cm^{-1} is also seen vaguely, although this excitation peak was not measured with good S/N ratios because of the low intensity. Further, the relative intensity of lower-energy peaks in the main $T_1(n, \pi^*)$ phosphorescence bands are found to increase with increasing temperature (Figure 5a). It is also seen in Figure 5b that the two peaks at 26 535 and 26 450 cm^{-1} in the fluorescence spectrum correspond well to the two peaks in the $S_0 \rightarrow S_1$ excitation origin.

The characteristic doublet-like bands observed in the $T_1(n, \pi^*) \rightarrow S_0$ phosphorescence and $S_0 \rightarrow S_1(n, \pi^*)$ excitation origin of 3-PCA vapor are assigned to the bands originating from the two different rotamers on the basis of the following observations: (1) Such a characteristic doublet-like structure is not observed in the phosphorescence and excitation spectra of 4-PCA vapor for which no stable rotamers exists. (2) The intensity of the lower-energy peaks in the main phosphorescence and excitation origin bands are too high to assign them as the combination bands and/or the hot band of the C═O stretching mode. (3) There is no vibrational modes showing 85 or 100 cm^{-1} in the calculated vibrational frequencies of 3-PCA in the ground state. (4) The observed temperature dependence of the emission and excitation spectra as well as the band locations are explained reasonably, if we assign the two peaks in the main

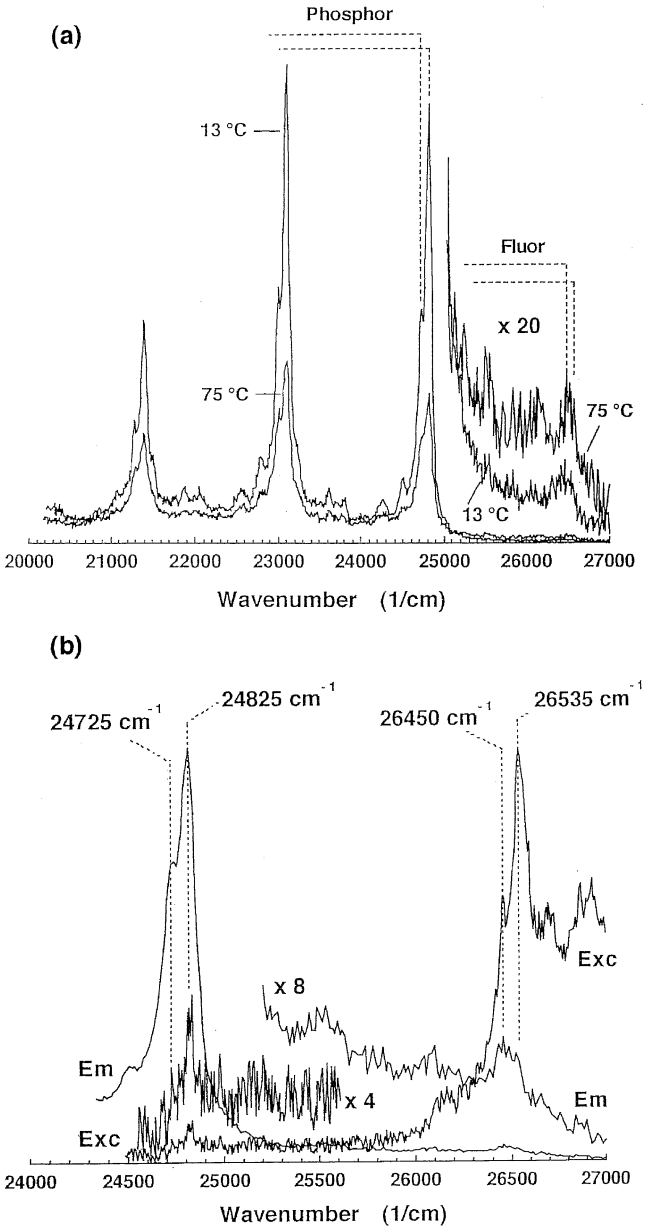

Figure 5. (a) Emission spectra of 3-PCA vapor in the presence of 280 Torr perfluorohexane at two different temperatures. (b) Emission and excitation spectra of 3-PCA vapor in the presence of perfluorohexane in an expanded scale, where the emission and excitation spectra are measured at 80 and 22 °C, respectively.

phosphorescence and excitation bands as those originating from the two different rotamers. This is discussed below in detail.

We have observed detectable temperature dependence of the intensities of the two peaks in the main phosphorescence bands of 3-PCA vapor (Figures 5a and 6a). To treat the observed band intensities quantitatively, the main phosphorescence bands were simulated by sum of Lorenztians, $\sum_i I(\nu_i)/[(\nu - \nu_i)^2 + b^2]$, where the parameters b and $I(\nu_i)$ were adjusted to fit the observed spectral patterns measured at different temperatures. The result of the simulation is shown also in Figure 6a. Although the observed phosphorescence spectra contain spectral congestion arising from the combination bands with the C═O stretching mode and the hot bands, the simulated spectra reproduce well the observed temperature dependence of the observed spectra. Using the integrated intensities of the Lorenztians, the logarithmic value of the intensity ratio of the two peaks (one at 24 825 cm^{-1} and other at 24 725 cm^{-1}) is plotted against $1/T$

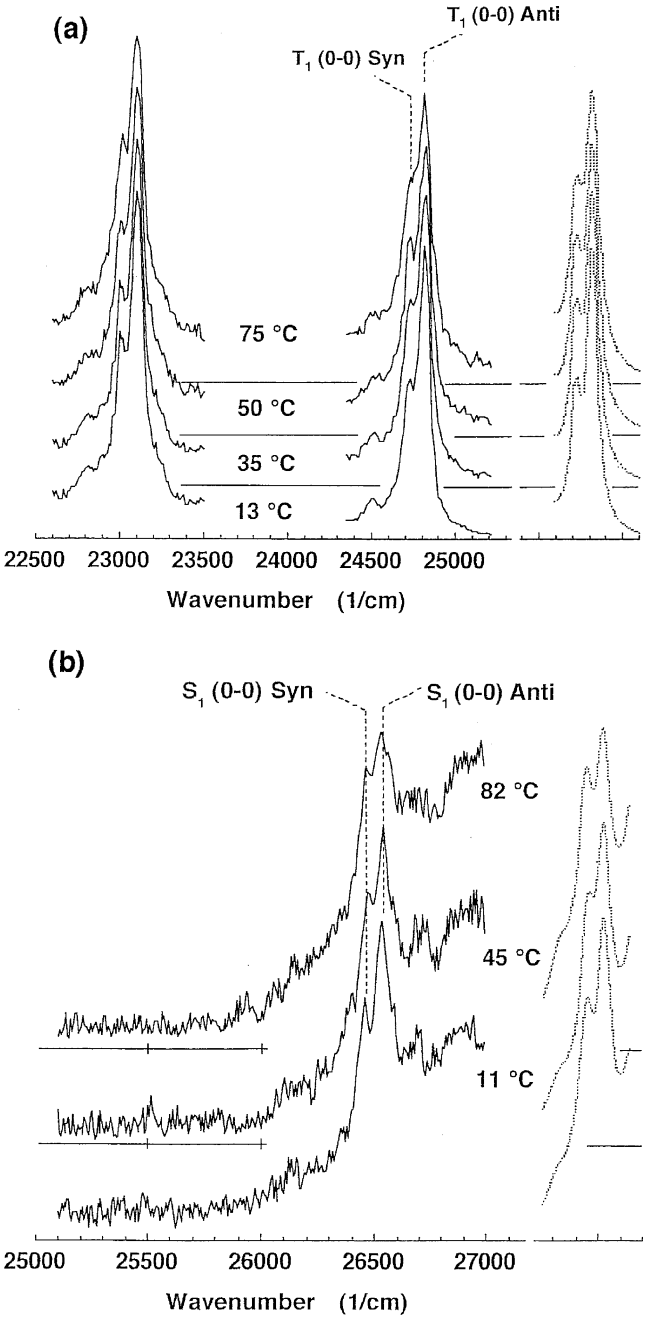

Figure 6. (a) Evolution of the main $T_1(n, \pi^*) \rightarrow S_0$ phosphorescence bands of 3-PCA vapor with varying temperature from 13 to 75 °C. Dotted-line spectra are calculated spectra. (b) Evolution of the $S_0 \rightarrow S_1$ (n, π^*) excitation origin band of 3-PCA vapor with varying temperature from 11 to 82 °C. Dotted-line spectra are calculated spectra.

(Figure 4). The energy difference obtained from the slope of the plots in Figure 4 is found to be 190 ± 30 cm^{-1}. Because the two peaks in the phosphorescence origin are separated by 100 cm^{-1}, the energy difference between the two rotamers in the ground state is evaluated to be 290 ± 30 cm^{-1} (=100 + 190 ± 30 cm^{-1}). The results of the DFT calculation show that the anti-rotamer is lower in energy than the syn rotamer by 222 cm^{-1} for 3-PCA in the ground state. This situation is supported also by the semiempirical SCF-MO calculations, although the calculated anti−syn energy difference in the ground state is somewhat small; 98 cm^{-1} with PM3, 56 cm^{-1} with MNDO and 65 cm^{-1} with AM1 calculation. Hence, the 24 825 and 24 725 cm^{-1} peaks in the phosphorescence origin of 3-PCA vapor are assigned, respectively, to those of the anti and syn rotamers,

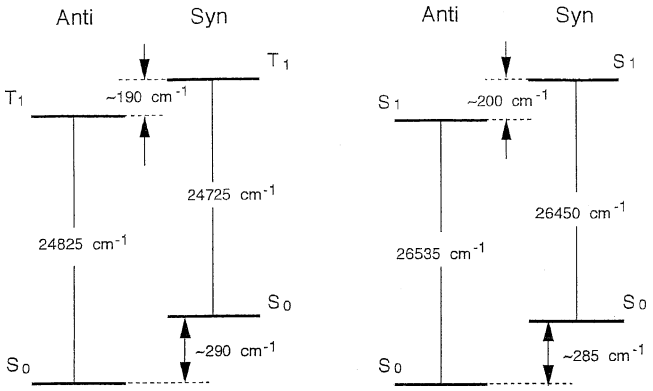

Figure 7. Energy diagrams showing the energy levels of the anti and syn rotamers in the ground, S_1 (left) and T_1 states (right) for 3-PCA vapor.

TABLE 3: Band Locations and the Assignments of the Emission Spectrum of 3-PCA Vapor

frequency (cm^{-1})	intensity[b]	assignment[c]	infrared[d]
26535	w	$S_1(0-0)$, anti	
26450	w	$S_1(0-0)$, syn	
26085	w	450, anti	448[e]
25830	w	705, anti	704
25415	w	1035, syn	1035, 1037
24825	vs	$T_1(0-0)$, anti	
24725	s	$T_1(0-0)$, syn	
24500	m	225, syn	222[e]
24285	m	440, syn	441[e]
24020	w	705, syn	703
23990	w	835, anti	834
23800	m	1025, anti	1024
23705	m	1020, syn	1022
23605	m	1120, syn	1119
23515	w	1210, syn	1206
23500	w	1325, anti	1325
23435	w	1390, anti	1388, 1385
23105	vs	1720, anti	1720
23000	s	1725, syn	1722
22775	m	1725 + 225, syn	
22560	m	1725 + 441, syn	
22270	w	1720 + 835, anti	
22080	m	1720 + 1025, anti	
21985	w	1720 + 1120, anti	
21880	m	1725 + 1120,syn	
21395	vs	1720 × 2, anti	
21285	s	1725 × 2, syn	

[a] The band locations have been determined with an accuracy of ±5 cm^{-1}. [b] vs, very strong; s, strong; m, medium; w, weak. [c] Only the vibrational frequencies in the ground state are indicated. As for vibrational assignments, see ref 19. [d] In Ar matrix at 13 K. [e] Obtained by DFT calculations, with the modification that the harmonic wavenumbers ν_{harm} were scaled by the relation, $\nu_{calc} = \nu_{harm} \times (0.9766 + 0.00000202 \times \nu_{harm})$, to reproduce the observed spectra (Yoshida, H.; Takeda, K.; Okamura, J.; Ehara, A.; Matsuura, H. *J. Phys. Chem. A* **2002**, *106*, 3580).

and we can draw an energy diagram as shown in Figure 7. Assignments of the peaks observed in emission spectrum of 3-PCA vapor are summarized in Table 3, where the bands for both the anti and syn rotamers are indicated. The fundamental frequencies of the C═O stretching mode in the phosphorescence spectra are found to be 1725 and 1720 cm^{-1} for the anti and syn rotamers, respectively, which agree well with those observed in the infrared spectrum in Ar (1722 and 1720 cm^{-1}, respectively).[19] The interval between the strong C═O stretching bands of the anti and syn rotamers, therefore, tends to separate from 100 to 105 and from 105 to 110 cm^{-1}, respectively, on going the vibrational quantum number from 0 to 1 and from 1 to 2.

The intensity of excitation spectrum reflects the relative populations of the closely located levels in the ground state. Figure 6b shows the $S_0 \rightarrow S_1$ excitation spectra of 3-PCA vapor near the origin measured at different temperatures. It is seen that the relative intensity of the lower-energy peak at 26 450 cm^{-1} increases with increasing temperature. To treat the band intensities quantitatively, the excitation spectrum is simulated by sum of Lorenztians in the same way already mentioned. The result of the simulation is shown also in Figure 6b. The simulated spectra reproduce the temperature dependence of the observed spectra well, and we obtained the energy difference of 285 ± 30 cm^{-1} through the logarithmic values of the intensity ratio of the two peaks plotted against $1/T$ (Figure 4). This energy difference agrees surprisingly well with that obtained from the temperature dependence of the phosphorescence spectrum (290 ± 30 cm^{-1}). Thus, we can conclude with a high reliability that the anti rotamer of 3-PCA vapor is lower in energy than the syn rotamer by 287.5 ± 32.5 cm^{-1} in the ground state. Further, because the energy difference between the two peaks in the $S_0 \rightarrow S_1$ excitation origin is 85 cm^{-1}, the energy difference between the two rotamers in the S_1 state is evaluated to be 200 ± 30 cm^{-1}, and we can draw also an energy diagram as shown in Figure 7.

The data in Table 3 show that the ΔE_{S-T} values are 1710 and 1725 cm^{-1}, respectively, for the anti and syn rotamers of 3-PCA vapor. The ΔE_{S-T} values can be evaluated also from the temperature dependence of the emission intensities, just as in the case of 2- and 4-PCA vapors. The ΔE_{S-T} and k_P/k_F values obtained from the logarithmic plots of I_P/I_F versus $1/T$ are respectively 1714 ± 40 cm^{-1} and 2.0×10^{-2} for the anti rotamers of 3-PCA vapor (Figure 4). These values are in excellent agreement with the ΔE_{S-T} value determined from the band positions and the $S_0 \rightarrow T_1/S_0 \rightarrow S_1$ origin-band intensity ratio in the absorption spectra in hexane (2.0×10^{-2}).[19] Although there are two peaks separated by 85 cm^{-1} corresponding to the two rotamers in the fluorescence origin, we could not carry out the quantitative analyses of the peak intensity of each rotamers because of the low intensity and spectral congestion.

4. Conclusions

It is shown that the emission spectra of 2-, 3- and 4-PCA vapors consist of the $T_1(n, \pi^*) \rightarrow S_0$ phosphorescence accompanied by the weak thermally activated $S_1(n, \pi^*) \rightarrow S_0$ delayed fluorescence. The S_1-T_1 energy separations obtained from the temperature dependence of the emission spectra agreed well with those obtained from the band positions for these molecules. With 3-PCA vapor, the peaks corresponding to the two rotamers were identified in the emission and excitation spectra. Temperature dependence of the relative intensity of the phosphorescence and excitation spectra of 3-PCA vapor provides the syn−anti energy difference of 290 ± 35 cm^{-1} in the ground state, 190 ± 40 cm^{-1} in the T_1 state, and 200 ± 30 cm^{-1} in the S_1 state. The syn−anti energy difference in the ground state is in reasonable agreement with the DFT output (222 cm^{-1}). The vibrational analysis of the emission spectrum and the DFT calculation demonstrated that the emission of 2-PCA vapor originates exclusively from the anti rotamer. Most of the observed main emission bands were reasonably assigned for all the molecules. 3-PCA is considered to be one of rare examples for which the two stable rotamers were identified in the emission and excitation spectra, and for which the energy difference between the two rotamers was determined in the ground and excited states.

Acknowledgments. The author is grateful to Professor Keiichi Ohno of Hiroshima University and to Dr. Motohiko Koyanagi for helpful information. This work was supported in part by a grant from Hiruma Fund (Phos Co.) in 2006 through the president of Hiroshima University.

References and Notes

(1) Lunazzi, L.; Macciantelli, D.; Cerioni, G. *J. Chem. Soc., Perkin Trans. 2* **1976**, 1791.
(2) Drakenberg, T. *J. Chem. Soc., Perkin Trans. 2* **1976**, 147.
(3) Danchura, W.; Schaefer, T.; Rowbotham, J. B.; Wood, D. J. *Can. J Chem.* **1974**, *52*, 3986.
(4) Kwiatkowski, J. S.; Swiderska M. *Bull. Acad Pol. Sci. Ser. Sci. Chim.* **1977**, *25*, 325.
(5) John I. G.; Ritchie, G. L. D.; Radom L. *J. Chem. Soc., Perkin Trans. 2* **1977**, 1601.
(6) Romani, A.; Bigozzi, A.; Ortica, F.; Favaro, G. *Spectrochim. Acta, Part A* **1999**, *55A*, 25.
(7) Ghoshal, S. K.; Sarkar, S. K. *Ind. Phys. B* **1984**, *58B*, 284.
(8) Padhye, M. R.; Jahagirdar, C. J. *Ind J. Chem.* **1975**, *13*, 1300.
(9) Latas, K. J.; Power, R. K.; Nishimura, A. M. *Chem. Phys. Lett.* **1979**, *65*, 272.
(10) Latas, K. J.; Nishimura, A. M. *J. Photochem.* **1978**, *9*, 577.
(11) Koyanagi, M.; Goodman, L. *Chem. Phys. Lett.* **1973**, *21*, 1.
(12) Kiritani, M.; Yoshii, T.; Hirota, N.; Baba, M. *J. Phys. Chem.* **1994**, *98*, 11265.
(13) Itoh, T. *Spectrochim. Acta, Part A* **2002**, *59A*, 61.
(14) Frisch, M. J.; Trucks, G. W.; Schlegel, H. B.; Scuseria, G. E.; Robb, M. A.; Cheeseman, J. R.; Montgomery, J. A., Jr.; Vreven, T.; Kudin, K. N.; Burant, J. C.; Millam, J. M.; Iyengar, S. S.; Tomasi, J.; Barone, V.; Mennucci, B.; Cossi, M.; Scalmani, G.; Rega, N.; Petersson, G. A.; Nakatsuji, H.; Hada, M.; Ehara, M.; Toyota, K.; Fukuda, R.; Hasegawa, J.; Ishida, M.; Nakajima, T.; Honda, Y.; Kitao, O.; Nakai, H.; Klene, M.; Li, X.; Knox, J. E.; Hratchian, H. P.; Cross, J. B.; Bakken, V.; Adamo, C.; Jaramillo, J.; Gomperts, R.; Stratmann, R. E.; Yazyev, O.; Austin, A. J.; Cammi, R.; Pomelli, C.; Ochterski, J. W.; Ayala, P. Y.; Morokuma, K.; Voth, G. A.; Salvador, P.; Dannenberg, J. J.; Zakrzewski, V. G.; Dapprich, S.; Daniels, A. D.; Strain, M. C.; Farkas, O.; Malick, D. K.; Rabuck, A. D.; Raghavachari, K.; Foresman, J. B.; Ortiz, J. V.; Cui, Q.; Baboul, A. G.; Clifford, S.; Cioslowski, J.; Stefanov, B. B.; Liu, G.; Liashenko, A.; Piskorz, P.; Komaromi, I.; Martin, R. L.; Fox, D. J.; Keith, T.; Al-Laham, M. A.; Peng, C. Y.; Nanayakkara, A.; Challacombe, M.; Gill, P. M. W.; Johnson, B.; Chen, W.; Wong, M. W.; Gonzalez, C.; Pople, J. A. *Gaussian 03*, revision C.02; Gaussian, Inc.: Wallingford, CT, 2004.
(15) MOPAC (CS Chem 3D Pro ver. 4.0); CambridgeSoft Co. MA, 1997.
(16) Becke, A. D. *J. Chem. Phys.* **1993**, *98*, 5648.
(17) Lee, C.; Yang, W.; Parr, R. G. *Phys. Rev. B* **1988**, *37*, 785.
(18) Stockburger, M. *Z. Phys. Chem.* **1962**, *31*, 350.
(19) Ohno, K.; Itoh, T.; Yokota. C.; Katsumoto, Y. *J. Mol. Struct.*, in press.